

RSC Advances



This is an *Accepted Manuscript*, which has been through the Royal Society of Chemistry peer review process and has been accepted for publication.

Accepted Manuscripts are published online shortly after acceptance, before technical editing, formatting and proof reading. Using this free service, authors can make their results available to the community, in citable form, before we publish the edited article. This *Accepted Manuscript* will be replaced by the edited, formatted and paginated article as soon as this is available.

You can find more information about *Accepted Manuscripts* in the [Information for Authors](#).

Please note that technical editing may introduce minor changes to the text and/or graphics, which may alter content. The journal's standard [Terms & Conditions](#) and the [Ethical guidelines](#) still apply. In no event shall the Royal Society of Chemistry be held responsible for any errors or omissions in this *Accepted Manuscript* or any consequences arising from the use of any information it contains.



Journal Name

ARTICLE

The grafting reaction of epoxidized natural rubber with carboxyl ionic liquids and the ionic conductivity of the solid electrolyte composites

Received 00th January 20xx,
Accepted 00th January 20xx

DOI: 10.1039/x0xx00000x

www.rsc.org/

Qiong Lin,^a Yanbo Lu,^a Wentan Ren,^{*b} Yong Zhang^a

Novel hybrid material were prepared by grafting reaction of 50 % epoxidized natural rubber (ENR 50) with 1-carboxymethyl-3-methylimidazoliumbis(trifluoromethylsulfonate) imine $[(\text{HOOC})\text{C}_1\text{C}_1\text{Im}][\text{NTf}_2]$. The grafting reaction and cross-linked structure of the hybrid material were investigated using the Attenuated total reflectance - Fourier transform infrared (ATR-FTIR) spectroscopy, Differential scanning calorimetry (DSC) and Equilibrium swelling method. The analysis results indicated that the carboxyl group of $[(\text{HOOC})\text{C}_1\text{C}_1\text{Im}][\text{NTf}_2]$ can react with the epoxy group of ENR 50 and generated ENR 50- $[(\text{HOOC})\text{C}_1\text{C}_1\text{Im}][\text{NTf}_2]$ graft polymer at the condition of 40 °C for 24 h. Furthermore, the grafting ENR 50 formed ionic clusters and led to ionic crosslinking. In addition, ENR 50/ $[(\text{HOOC})\text{C}_1\text{C}_1\text{Im}][\text{NTf}_2]$ /LiTFSI electrolyte composites were prepared through introducing bis(trifluoromethanesulfon) imide lithium salt (LiTFSI) into the ENR 50/ $[(\text{HOOC})\text{C}_1\text{C}_1\text{Im}][\text{NTf}_2]$ hybrid system and the ionic conductivity of the electrolyte composites were studied. The results showed that the electrolyte composites have high ionic conductivity and reached a maximum ionic conductivity of $3.01 \text{ E-04 S cm}^{-1}$ (23 °C) in the experimental range.

1. INTRODUCTION

Epoxidized natural rubber (ENR) is one of the modified natural rubber. ENR has distinctive characteristics such as low glass transition temperature (T_g), good elasticity and adhesion properties.¹ Furthermore, ENR has a polar group in their epoxy ring that will provide coordination sites for Li^+ conduction. And epoxy group in ENR can react with other groups like carboxyl group and amine group.

Ionic liquids (ILs) are molten liquids at room temperature with low melting point.² They are composed of bulky cations and anions and are considered as promising green electrolytes due to their unique and excellent characteristics such as negligible vapour pressure, non-flammability, non-corrosive with high thermal stability which makes them suitable for numerous applications,^{3,4} e.g. solvents in preparative chemistry and electrolytes in lithium batteries. In general, functional ionic liquids (FILs) are designed and synthesized by attachment of functional groups onto the side chains of ILs. Such chemical functionalization usually enhances the versatility of ILs, thereby leading to a large number of diverse FILs with improved properties.^{5,6}

It is reported that the ILs is used as plasticizers of solid polymer

electrolyte (SPE) or gel polymer electrolytes (GPE) in the recent literature,⁷⁻⁹ and most of the related publication focused on the physical blends of ILs and polymer matrix. However, some of our previous publications concern with the SPE and GPE preparation by ILs compounded with rubbers,^{10,11} the results showed that the ILs was easy to be migration from the polymer matrix and resulted in instability of ionic conductivity and poor mechanical properties due to the compatibility problem between the ILs and polymer matrix when ILs content increasing. In this work, the carboxyl ionic liquids $[(\text{HOOC})\text{C}_1\text{C}_1\text{Im}][\text{NTf}_2]$ was grafted on 50% epoxidized natural rubber (ENR 50) chains through reaction between the carboxyl group of $[(\text{HOOC})\text{C}_1\text{C}_1\text{Im}][\text{NTf}_2]$ and the epoxy group of ENR 50. Thereby, it formed ionic crosslinking of ENR 50 chains and ENR 50/ $[(\text{HOOC})\text{C}_1\text{C}_1\text{Im}][\text{NTf}_2]$ hybrid material were prepared. The grafting reaction and cross-linked structure of the hybrid material were investigated using the ATR-FTIR, DSC and equilibrium swelling method. Furthermore, ENR 50/ $[(\text{HOOC})\text{C}_1\text{C}_1\text{Im}][\text{NTf}_2]$ /LiTFSI electrolyte composites were prepared through introducing bis(trifluoromethanesulfonyl) imide lithium salt (LiTFSI) into the ENR 50/ $[(\text{HOOC})\text{C}_1\text{C}_1\text{Im}][\text{NTf}_2]$ hybrid system and the ionic conductivity of the electrolyte composites was studied.

2. Experimental

2.1 Materials

ENR was the epoxidized natural rubber with 50% epoxidation and trade name ENR 50, produced by Chinese Academy of

^a School of Chemistry and Chemical Engineering, Shanghai Jiao Tong University, Shanghai 200240, People's Republic of China. E-mail: junelin0626@sjtu.edu.cn; tel: +86021-5474-3261

^b School of Chemistry and Chemical Engineering, Shanghai Jiao Tong University, Shanghai 200240, People's Republic of China. E-mail: 1958rwt@sjtu.edu.cn; tel: +86021-5474-2671

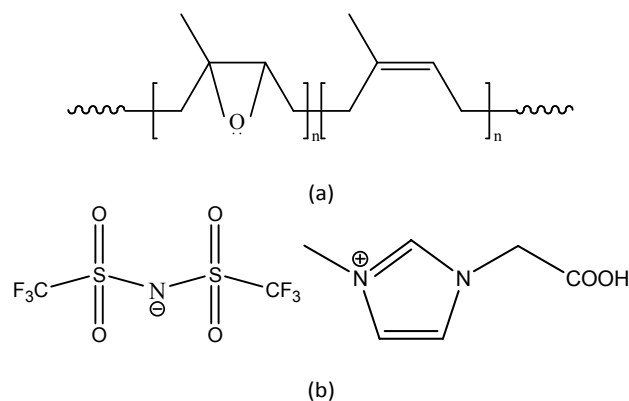


Figure 1. Structure of ENR 50 and $[(\text{HOOC})\text{C}_1\text{C}_1\text{Im}][\text{NTf}_2]$.

Tropical Agricultural Sciences (CATAS, Hainan, China) and its structure is shown in Fig. 1(a). 1-carboxymethyl-3-methylimidazolium bis(trifluoromethylsulfonate)imide ($[(\text{HOOC})\text{C}_1\text{C}_1\text{Im}][\text{NTf}_2]$) and bis(trifluoromethanesulfonyl)imide lithium salt (LiTFSI) were purchased from Lanzhou Institute of Chemical Physics (LICP, Lanzhou, China), its structure is shown in Fig. 1(b). All solvents including tetrahydrofuran (THF), xylene and toluene were supplied by Sinopharm Chemical Reagent Co. Ltd, China.

2.2 Sample preparation

ENR 50 was first dissolved in toluene and precipitated in methanol for purification. According to the predetermined proportion, the purified ENR 50 and $[(\text{HOOC})\text{C}_1\text{C}_1\text{Im}][\text{NTf}_2]$ were dissolved in a mixed solvent (the volume ratio of THF and xylene is 3/2) and THF, respectively. Then these two solutions were mixed and stirred efficiently for 2 h at room temperature to achieve a homogenous mixture. The solution was then poured into Teflon® moulds protected from dust which were subsequently dried at room temperature for 12 h to evaporate residual solvent. Further drying of the various solutions were continued in a vacuum oven under 40 °C for 24 h. The samples were stored in a desiccator until further usage.

The extraction procedure of crosslinked rubber: the samples were first immersed in toluene for several days until they reached equilibrium weights. During these days toluene was changed to a new one every day. Then the samples were dried in vacuum oven under 40 °C until equilibrium weights again. The similar approach was used to prepare the ENR solid electrolyte composites with various content of LiTFSI.

2.3 Characterization

2.3.1 ATR-FTIR spectroscopy. ATR-FTIR analysis was carried out using Perkin-Elmer Spectrum 1000 in the range of wave numbers 4000 to 650 cm^{-1} at room temperature with scanning resolution of 4 cm^{-1} . In order to remove the unreacted $[(\text{HOOC})\text{C}_1\text{C}_1\text{Im}][\text{NTf}_2]$, the sample would be extracted in toluene at 25 °C for 3 days before ATR-FTIR testing.

2.3.2 DSC characterization. DSC analysis was by two methods. DSC characterization was performed using a TA Q2000 instrument (TA Instruments, USA). In the first method, samples

of compounds of ENR 50 and $[(\text{HOOC})\text{C}_1\text{C}_1\text{Im}][\text{NTf}_2]$ were sealed in hermetic aluminum pans and scanned at a heating rate of 10 °C min^{-1} under a nitrogen flow at a rate of 50 ml min^{-1} . In each case, using the following cycle: quenching from room temperature to -80 °C, heating at a rate of 20 °C min^{-1} to 120 °C, quenching at 10 °C min^{-1} to -80 °C and heating at the same rate of 10 °C min^{-1} up to 120 °C. The second method was used to study the kinetics of the modification reaction. The mixed solution of ENR 50 and $[(\text{HOOC})\text{C}_1\text{C}_1\text{Im}][\text{NTf}_2]$ was first removed of solvent by pumping. Then samples of approximately 10 mg in weight were sealed in hermetic aluminum pans and scanned at heating rates of 5, 7.5, 10 and 15 °C/min under a nitrogen flow of 50 ml/min . The data were analysed using the Universal Analysis 2000 software provided by TA instruments.

2.3.3 Determination of crosslink density. The crosslink density of ENR 50/ $[(\text{HOOC})\text{C}_1\text{C}_1\text{Im}][\text{NTf}_2]$ hybrid materials was determined by Equilibrium swelling method.¹² The samples were first weighed for initial dry weights and then inserted into bottles containing 50 ml toluene at 23 °C for several days until achieved a swelling equilibrium. The samples were removed from the solvent and blotted with filter paper to remove excess solvent from the surface of the sample, then weighed for the equilibrium weights. The samples then were dried in oven under 80 °C for 24 hours and reweighed for the final dry weights. The crosslinking density have been calculated from the Flory-Rehner equation¹³:

$$v_e = -\frac{1}{v} \left[\frac{\ln(1-v_2) + v_2 + \chi v_2^2}{v_2^{1/3}} \right] \quad (1)$$

Where v_e is the crosslinking density (in mole per unit volume), v is the molar volume of the solvent, v_2 is the volume fraction of the polymer in the swollen mass and calculated as equation (2), χ is the Flory-Huggins polymer-solvent interaction parameter and calculated as equation (3).

$$dv_2 = \frac{m_3/\rho}{\frac{m_3}{\rho} + \frac{m_2 - m_1}{\rho_s}} \quad (2)$$

where m_1 is the mass of the sample before swelling, m_2 is the swollen mass of the sample when swelling equilibrium, m_3 is the mass of sample after final drying in oven, ρ is the density of polymer and ρ_s is the density of the solvent.

$$\chi = \frac{v}{RT} (\delta_1 - \delta_2)^2 \quad (3)$$

where R is the gas constant, δ_1 is the solubility parameter of solvent and δ_2 is the solubility parameter of polymer.

2.3.4 Mechanical properties. The stress-strain tests were performed with a universal material testing machine (Instron 4465, Instron Corp, USA) with a cross-head speed of 500 mm/min according to the standard ASTM D412-06a. To measure the mechanical properties, five different dumbbell-shaped specimens were punched from each rubber sample. Tensile strength and elongation at break were measured at room temperature.

2.3.5 Determination of the ionic conductivity. The ionic conductivity determination of ENR solid electrolyte composites was carried out using Autolab PGSTA302 in the frequency range of 1 Hz - 1 MHz with a 10 mV amplitude at room temperature. The polymer solid electrolyte was sandwiched

between the stainless steel ion-blocking electrodes with a surface contact area of 0.25 cm^2 . The bulk resistance (R_b) was determined from the equivalent circuit analysis. The conductivity values (σ) have been calculated from the equation $\sigma = d \cdot R_b^{-1} \cdot S^{-1}$, where d is the sample thickness and S is the active area of the electrode (cm^2).

3. Results and discussion

3.1 ATR-FTIR analysis

The grafting reaction of ENR 50 with $[(\text{HOOC})\text{C}_1\text{C}_1\text{Im}][\text{NTf}_2]$ was confirmed by ATR-FTIR spectra as shown in Figure 2. Figure 2 (a) through (c) show the ATR-FTIR spectra of ENR 50 gum, $[(\text{HOOC})\text{C}_1\text{C}_1\text{Im}][\text{NTf}_2]$ and ENR 50/ $[(\text{HOOC})\text{C}_1\text{C}_1\text{Im}][\text{NTf}_2]$ reaction products, respectively. ENR 50 has the absorption peaks with the basic characteristics of natural rubber, such as C-H stretching mode at 2960 and 2920 cm^{-1} , $\text{C}=\text{C}$ stretching mode at 1651 cm^{-1} and CH_2 scissoring mode at 1451 cm^{-1} .

The characteristic absorption peak of ENR 50 is the C-O-C stretching from the epoxy ring mode at 873 cm^{-1} . The characteristic absorption peaks corresponding to the carboxyl group of $[(\text{HOOC})\text{C}_1\text{C}_1\text{Im}][\text{NTf}_2]$ are 3300 , 1743 and 974 cm^{-1} , which are attributed to free carboxyl O-H, C=O and C-O stretching vibration, respectively. The absorption peaks at 3160 cm^{-1} and 3170 cm^{-1} are assigned to the stretching vibration of C-H bond on the imidazole ring. The absorption peaks at 1576 cm^{-1} and 1174 cm^{-1} are assigned to the framework vibration of the imidazole ring and the bending vibration of C-H bond on the imidazole ring, the absorption peaks at 1347 cm^{-1} and 1131 cm^{-1} are assigned to the characteristic absorption of $-\text{CF}_3$ group and the absorption peaks at 1052 cm^{-1} is assigned to the characteristic absorption of $-\text{SO}_2-\text{N}-\text{SO}_2-$ group. As is shown in Figure 2 (c), when the ENR 50 and $[(\text{HOOC})\text{C}_1\text{C}_1\text{Im}][\text{NTf}_2]$ were mixed, reacted and extraction processed, the characteristic absorption peaks corresponding to the carboxyl group of $[(\text{HOOC})\text{C}_1\text{C}_1\text{Im}][\text{NTf}_2]$ (1743 cm^{-1} and 974 cm^{-1}) and the epoxy ring group of ENR 50 (873 cm^{-1}) were almost disappeared on the ATR-FTIR spectra of ENR 50/ $[(\text{HOOC})\text{C}_1\text{C}_1\text{Im}][\text{NTf}_2]$ reaction products, and new absorption band is observed around 3401 cm^{-1} and 1718 cm^{-1} , which are attributed to hydroxyl groups (-OH) and the ester C=O bonds, respectively.

Figure 3 shows the effect of $[(\text{HOOC})\text{C}_1\text{C}_1\text{Im}][\text{NTf}_2]$ content on the ENR 50/ $[(\text{HOOC})\text{C}_1\text{C}_1\text{Im}][\text{NTf}_2]$ reaction products and all ATR-FTIR spectra were baseline corrected and normalized using the aliphatic methylene bending peak at 1449 cm^{-1} . Also, the unreacted $[(\text{HOOC})\text{C}_1\text{C}_1\text{Im}][\text{NTf}_2]$ in the samples are removed by the extraction processing. As shown in figure 3, with increasing of $[(\text{HOOC})\text{C}_1\text{C}_1\text{Im}][\text{NTf}_2]$ content, the absorption peaks corresponding to $-\text{OH}$ (3401 cm^{-1}) is shifted to low wavenumber and divided into two absorption peaks, the absorption peaks corresponding to the ester C=O bonds is shifted to 1697 cm^{-1} from 1718 cm^{-1} . This implies that the effect of hydrogen bonded becomes more intense with increasing $[(\text{HOOC})\text{C}_1\text{C}_1\text{Im}][\text{NTf}_2]$ content. Furthermore, the

increasing $[(\text{HOOC})\text{C}_1\text{C}_1\text{Im}][\text{NTf}_2]$ content led to that the C-O-C stretching from the epoxy ring mode (873 cm^{-1}) show subtle

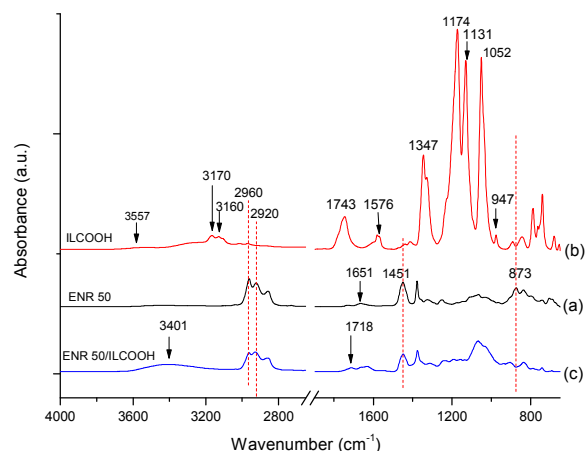


Figure 2. ATR-FTIR spectra of purified ENR 50, pure $[(\text{HOOC})\text{C}_1\text{C}_1\text{Im}][\text{NTf}_2]$ and ENR 50/ $[(\text{HOOC})\text{C}_1\text{C}_1\text{Im}][\text{NTf}_2]$ reaction products

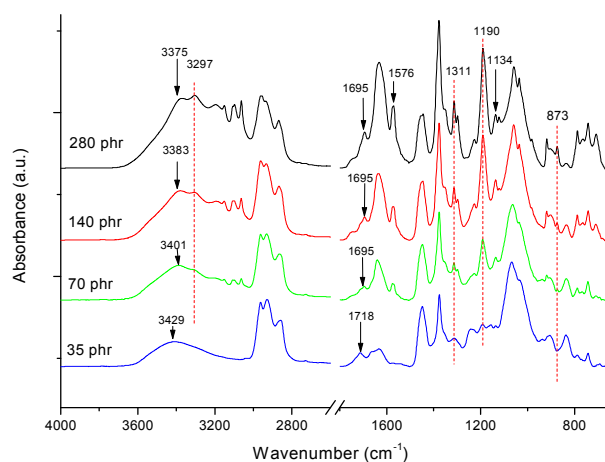
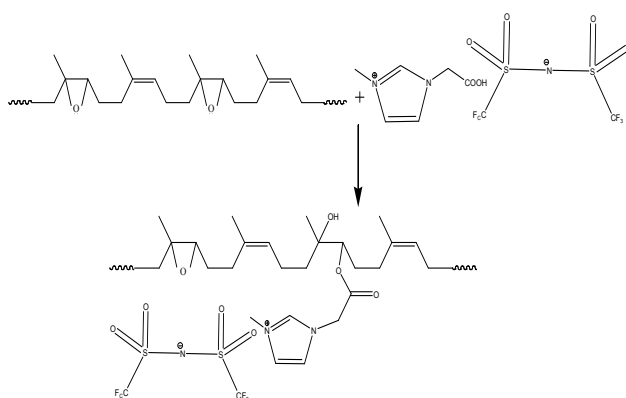


Figure 3. ATR-FTIR spectra of pure ENR 50, and ENR 50 with various content of $[(\text{HOOC})\text{C}_1\text{C}_1\text{Im}][\text{NTf}_2]$ dried under $40 \text{ }^\circ\text{C}$ after extraction



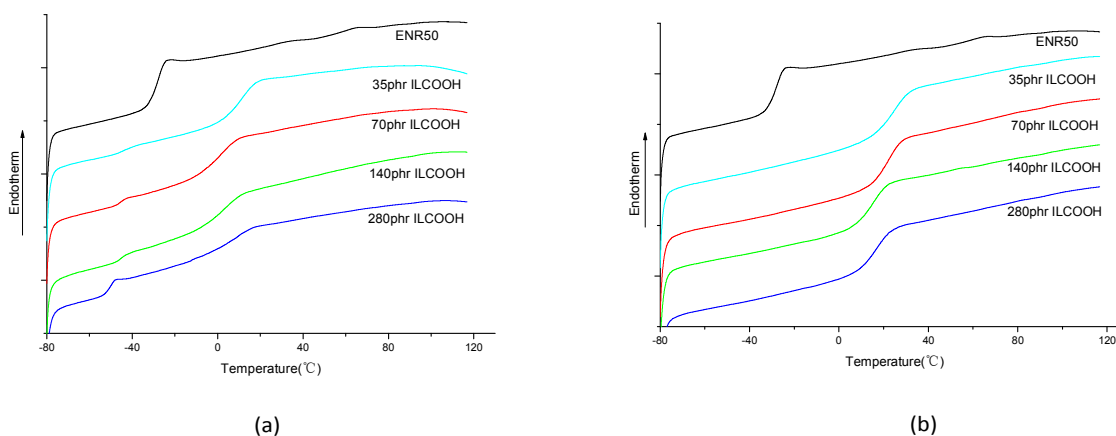
Scheme 1. Reaction of ENR 50 with $[(\text{HOOC})\text{C}_1\text{C}_1\text{Im}][\text{NTf}_2]$

change, scilicet, the conversion rate of epoxy groups first increased then decreased (as shown in Table 1). This result is mainly due to that the aggregation or clusters of ionic liquids ($[(\text{HOOC})\text{C}_1\text{C}_1\text{Im}][\text{NTf}_2]$) formed with the increasing solution concentration in the process of sample preparation, thus aroused its grafting reaction efficiency decreased.¹⁶ Besides that, the absorption peaks corresponding to the framework vibration and C-H stretching vibration of imidazole ring is emergence and shifting to low wavenumber, the characteristic

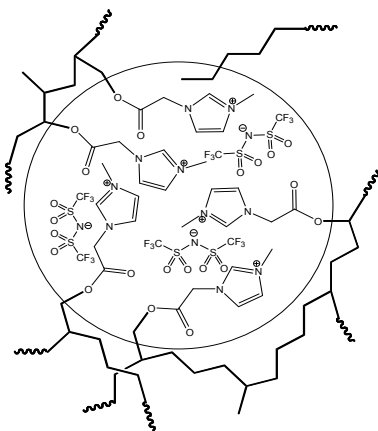
absorption of $-\text{CF}_3$ and $-\text{SO}_2\text{-N-SO}_2-$ group have faint enhancement and faintly appeared the carboxyl group peaks (1743 cm^{-1}) with the $[(\text{HOOC})\text{C}_1\text{C}_1\text{Im}][\text{NTf}_2]$ content increased. This should be due to the aggregation or cluster effects of the ionic liquid, make that unreacted $[(\text{HOOC})\text{C}_1\text{C}_1\text{Im}][\text{NTf}_2]$ cannot be completely removed from the samples.¹⁷ The above results are evident that consumption of epoxy groups is accompanied by formation of hydroxyl groups and ester groups, which further suggests that the ENR 50 and the

Table 1. The conversion rate of epoxy groups with different $[(\text{HOOC})\text{C}_1\text{C}_1\text{Im}][\text{NTf}_2]$ content

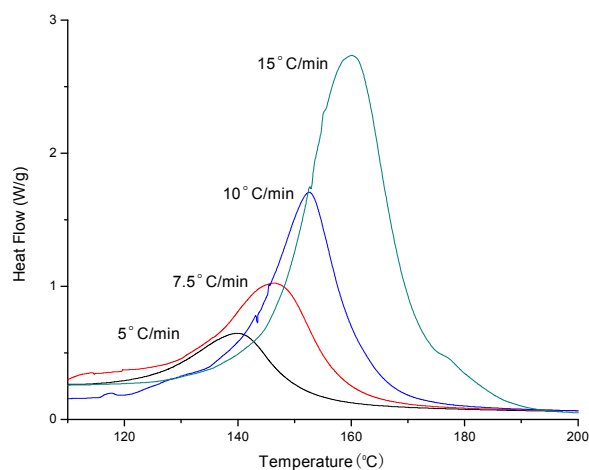
$[(\text{HOOC})\text{C}_1\text{C}_1\text{Im}][\text{NTf}_2]$ (phr)	The peak area of $\nu(\text{epoxy ring})$	The conversion rate of epoxy groups, %
0	0.325	0
35	0.075	76.80
70	0.061	81.10
140	0.057	82.42
280	0.111	65.89

Figure 4. DSC thermographs of pure ENR 50, and ENR 50/ $[(\text{HOOC})\text{C}_1\text{C}_1\text{Im}][\text{NTf}_2]$ reaction products with various content of $[(\text{HOOC})\text{C}_1\text{C}_1\text{Im}][\text{NTf}_2]$: (a) without extraction, (b) with extractionTable 2. The T_g of samples with various content of $[(\text{HOOC})\text{C}_1\text{C}_1\text{Im}][\text{NTf}_2]$

$[(\text{HOOC})\text{C}_1\text{C}_1\text{Im}][\text{NTf}_2]$ (phr)	the T_g values of samples without extraction, °C	the T_g values of samples with extraction, °C
0	-31.89	-31.89
35	3.45	16.61
70	-6.58	15.84
140	-6.89	8.34



Scheme 2. Schematic diagram of the ionic cluster structure

Figure 5. Nonisothermal dynamic DSC curves of ENR 50-[(HOOC)C₁C₁Im][NTf₂] with 70 phr [(HOOC)C₁C₁Im][NTf₂].Table 3. Values of Activation Energy and *n* for ENR 50-[(HOOC)C₁C₁Im][NTf₂] with different content of [(HOOC)C₁C₁Im][NTf₂] during dynamic curing processes

	Kissinger	Flynn-Wall-Ozawa
--	-----------	------------------

[(HOOC)C₁C₁Im][NTf₂] take place the grafting reaction as shown in Scheme 1.

3.2 DSC characterization

Figure 4 shows DSC thermographs obtained at a heating rate of 10 °C min⁻¹ for ENR 50/[(HOOC)C₁C₁Im][NTf₂] reaction products. Two endotherms are observed in figure 4 (a) while there is only one endotherm in figure 4 (b) for the sample of identical [(HOOC)C₁C₁Im][NTf₂] content.

As Figure 4 (a) shown, two endothermic peaks are observed at -31.89 °C and -41.37 °C, which are assigned to the glass transition temperature (*T_g*) of the pure ENR 50 and [(HOOC)C₁C₁Im][NTf₂], respectively. The *T_g* values of ENR 50/[(HOOC)C₁C₁Im][NTf₂] reaction products with various content of [(HOOC)C₁C₁Im][NTf₂] would be calculated by the Figure 4 and the results are displayed in Table 2, it can be seen that the *T_g* values of ENR 50/[(HOOC)C₁C₁Im][NTf₂] reaction products with various content of [(HOOC)C₁C₁Im][NTf₂] increased about 25 °C then the pure ENR 50, while the *T_g* shifts into lower temperature with increasing [(HOOC)C₁C₁Im][NTf₂] content. The results can be considered to that the ENR 50/[(HOOC)C₁C₁Im][NTf₂] reaction products, namely, the hydroxy esters macromolecules with ionic side group formed the ionic clusters,¹⁸⁻²¹ and result in ENR 50 crosslink as the Scheme 2 base on ATR-FTIR analysis. Gan S N et al.²² thought that the significant elevation of *T_g* associated with ENR vulcanized by dibasic acids is probably predominantly due to the modified main chain structure rather than the crosslinking network. However, with increasing [(HOOC)C₁C₁Im][NTf₂] content, the side group in grafted ENR 50 increase and the chains regularity are reduced, thereby the ionic crosslinking will be inhibited. In addition, the *T_g* of the samples with extraction are higher than the samples without extraction where the unreacted [(HOOC)C₁C₁Im][NTf₂] played as a plasticizer.

Multiple-heating-rate methods are iso-conversion methods, that is, it assumes that the conversion value is constant at the

(HOOC) ₂ C ₁ C ₁ Im][NTf ₂] (phr)	E _{Kissinger} ^a (kJ/mol)	lnA	R-square	E _{Flynn} ^b (kJ/mol)	lnA	R-square
35	63.79	17.93	0.9981	67.09	19.34	0.9983
70	72.95	19.88	0.9955	76.07	21.10	0.9963
140	76.57	21.74	0.9901	79.28	22.81	0.9912
280	73.84	21.34	0.9224	76.58	22.44	0.9341

^aE_{Kissinger}: activation energy obtained from Kissinger method.

^bE_{Flynn}: activation energy obtained from Flynn-Wall-Ozawa method.

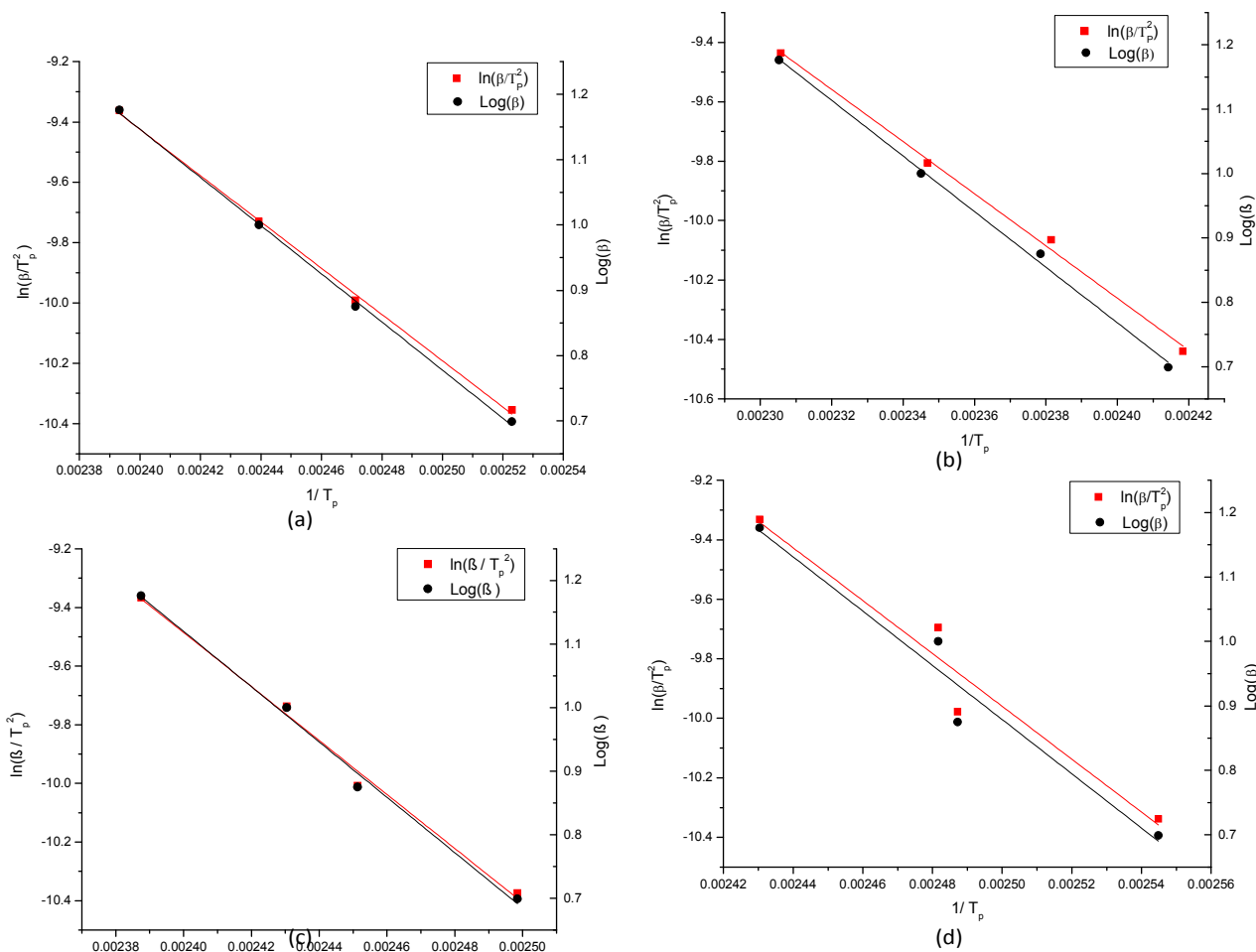


Figure 6. Plots of $\ln(\beta/T_p^2)$ and $\log(\beta)$ versus $1/T_p$ of ENR 50-[(HOOC)₂C₁C₁Im][NTf₂] with different content of [(HOOC)₂C₁C₁Im][NTf₂] during dynamic curing processes: (a) 35 phr; (b) 70 phr; (c) 140 phr; (d) 280 phr.

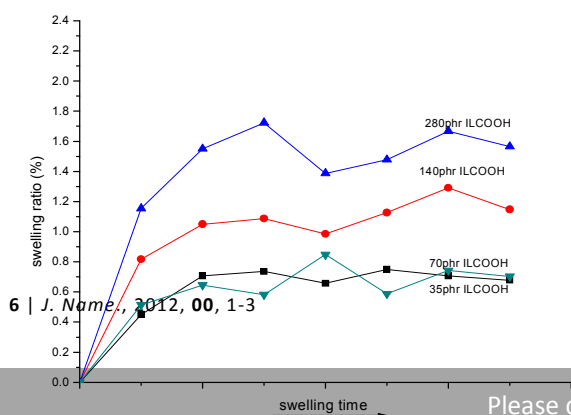


Figure 7. The swelling ratio of the ENR 50/[(HOOC)₂C₁C₁Im][NTf₂] reaction products with various [(HOOC)₂C₁C₁Im][NTf₂] content (the samples with extraction)

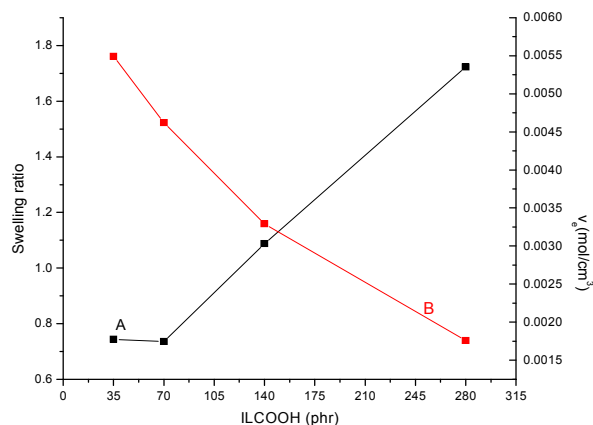


Figure 8. (A) swelling ratio; (B) crosslinking density of ENR 50/[(HOOC)C₁C₁Im][NTf₂] reaction products after extraction

peak exotherm temperature, the extent of reaction at the peak exotherm (α_p) in a DSC analysis, and is independent of the heating rate²³. This makes it equally effective for both the n th order and the autocatalytic reactions. Two such multiple heating rate methods that have been shown to be effective are that proposed by Ozawa²⁴ and Flynn and Wall²⁵, and that proposed earlier by Kissinger²⁶⁻²⁷.

From the peak temperature-heating-rate data, the evaluation of the reaction activity and reaction order was provided regardless of the reaction process with the following Kissinger equation and Flynn–Wall–Ozawa equation, respectively:

$$\frac{d[\ln(\beta/T_p^2)]}{d(1/T_p)} = -\frac{E}{R} \quad (4)$$

where β is the heating rate (kelvin per minute), T_p is the peak endotherm temperature (kelvin), and R the universal gas constant (8.314 J/mol/K). It is simplistic to assume a single reaction occurring during the curing process given the complexity of the reaction. Thus the value of E obtained in Eq. (4) is an overall value representing all complex reactions that occur during curing.

Flynn–Wall–Ozawa methods

$$\log(\beta) = \log\left[\frac{AE}{R}\right] - 2.315 - \frac{0.457E}{RT_p} \quad (5)$$

where A is the frequency factor.

The average values of activation energy with between the Kissinger and Flynn–Wall–Ozawa methods were introduced into the following the Crane²⁸ equation:

$$\left[\frac{d(\ln \beta)}{d(1/T_p)}\right] = -\left(\frac{E}{nR} + 2T_p\right) \quad (6)$$

where n is reaction order when $E/nR \gg 2T_p$ is founded; the equation is simplified into

$$\left[\frac{d(\ln \beta)}{d(1/T_p)}\right] = -\left(\frac{E}{nR}\right) \quad (7)$$

Therefore, a plot of $\ln \beta$ versus $1/T_p$ gives E .

The samples with various of [(HOOC)C₁C₁Im][NTf₂] were tested at four heating rates carried out in DSC, and the curves of ENR 50-[(HOOC)C₁C₁Im][NTf₂] with 70 phr [(HOOC)C₁C₁Im][NTf₂], are shown in Figure 5. Applying Kissinger and Flynn–Wall–Ozawa methods to the maximum reaction rate, linear relationships were obtained by plotting $\ln \beta/T_p^2$ against $1/T_p$, and $\log(\beta)$ confirming the validity of the models. The plots for all samples were given in Figure 6. Table 3 summarizes the obtained kinetic parameters and coefficient of correlation (R -square) for all samples. And the overall reaction order, n , were shown in Table 4. As shown in Table 3, the values of E are respectively, 63.79–76.51 and 67.09–79.28 kJ/mol by using Kissinger and Flynn–Wall–Ozawa methods, which are in agreement with the values of early literature²⁹. From Table 3, the values obtained by the Kissinger methods are slightly lower the trend of the change of values is similar. The activation than those obtained by the Flynn–Wall–Ozawa methods, but energy first showed an increase then has a slight decrease with the increasing of [(HOOC)C₁C₁Im][NTf₂], which means that too much more [(HOOC)C₁C₁Im][NTf₂] will hinder the reaction. This may because the viscosity effects the curing rate during the curing process of thermosetting resin³⁰. The more [(HOOC)C₁C₁Im][NTf₂], the more viscous the system is. And as the reaction proceeds, three-dimension crosslinking occurred, and the systems became dense that increase the viscosity and hinder the reaction.

3.3 The crosslink density

The swelling of crosslinking polymer involves a diffusion process of the liquid in polymer samples. Therefore, the swelling properties are closely related to the crosslinking density of polymer, and the swelling ratio and swelling rate would be decrease with increasing crosslinking density.³¹⁻³³

The swelling ratio was estimated as³⁴

$$S_w = \frac{W_t - W_0}{W_0} \quad (8)$$

where W_0 is the weight of the dry sample, and W_t is the weight of the swollen sample.

Table 4. Values of the Overall Reaction Order, n obtain from the Crane method.

(HOOC)C ₁ C ₁ Im][NTf ₂] (phr)	$n_{\text{Kissinger}}^a$	n_{Flynn}^b
35	0.90	0.95
70	0.91	0.95
140	0.90	0.94
280	0.85	0.88

^a $n_{\text{Kissinger}}$: using the value of E obtained from Kissinger method.

^b n_{Flynn} : using the value of E obtained from Flynn–Wall–Ozawa method

Table 5. The crosslink density of samples with various [(HOOC)C₁C₁Im][NTf₂] content

$[(\text{HOOC})\text{C}_1\text{C}_1\text{Im}][\text{NTf}_2]$ (phr)	The equilibrium swelling ratio (%)	The crosslink density (mol/cm^3)
0	—	0
35	0.74	0.0055
70	0.73	0.0046
140	1.09	0.0033
280	1.72	0.0017

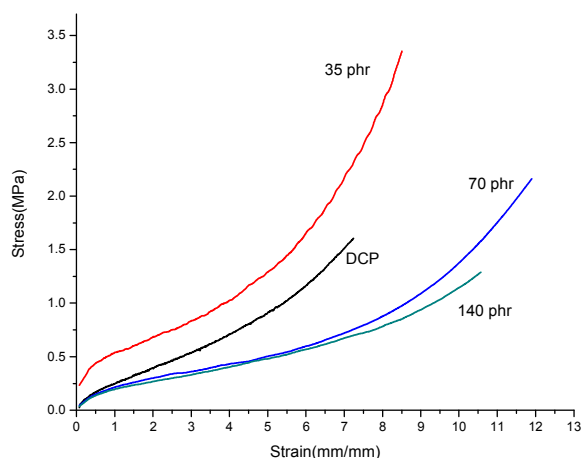


Figure 9. Strain-stress graph of samples with different content of $[(\text{HOOC})\text{C}_1\text{C}_1\text{Im}][\text{NTf}_2]$.

Figure 7 shows the effect of $[(\text{HOOC})\text{C}_1\text{C}_1\text{Im}][\text{NTf}_2]$ content on the swelling process and it is observed that the swelling ratio and swelling rate increase with increasing $[(\text{HOOC})\text{C}_1\text{C}_1\text{Im}][\text{NTf}_2]$ content. The equilibrium swelling ratios are estimated on the basis of the experimental data as shown in Figure 8 and the crosslink density of samples are calculated by the equation (1) based on the swelling testing. Table 5 enumerates the equilibrium swelling ratio and the crosslink density of samples with various $[(\text{HOOC})\text{C}_1\text{C}_1\text{Im}][\text{NTf}_2]$ content, the results indicate that the crosslinking density of ENR 50/ $[(\text{HOOC})\text{C}_1\text{C}_1\text{Im}][\text{NTf}_2]$ reaction products with various $[(\text{HOOC})\text{C}_1\text{C}_1\text{Im}][\text{NTf}_2]$ content decreases with the increasing $[(\text{HOOC})\text{C}_1\text{C}_1\text{Im}][\text{NTf}_2]$ content. The results are consistent with the T_g 's varying pattern attained by DSC characterization.

3.4 Mechanical properties

The influence of $[(\text{HOOC})\text{C}_1\text{C}_1\text{Im}][\text{NTf}_2]$ content on mechanical properties of ENR 50/ $[(\text{HOOC})\text{C}_1\text{C}_1\text{Im}][\text{NTf}_2]$ composites are illustrated in figure 9 and table 6. It was expected that the mechanical properties of the composites would be enhanced due to the crosslinking. As shown, the tensile strength showed a downward trend with increasing amount of $[(\text{HOOC})\text{C}_1\text{C}_1\text{Im}][\text{NTf}_2]$. While the elongation at break first

increased then decreased. And it reached a maximum value of 1190% with 70 phr ILCOOH. When adding a lot ILCOOH into ENR 50 caused a dilution effect³⁵, i.e. the volume fraction of rubber matrix decreased with increasing ILCOOH loading, which would lead to a decrease of crosslinking of composites and then a decrease of the elongation at break.³⁶ These results are consistent with both DSC and crosslinking.

3.5 The ionic conductivity

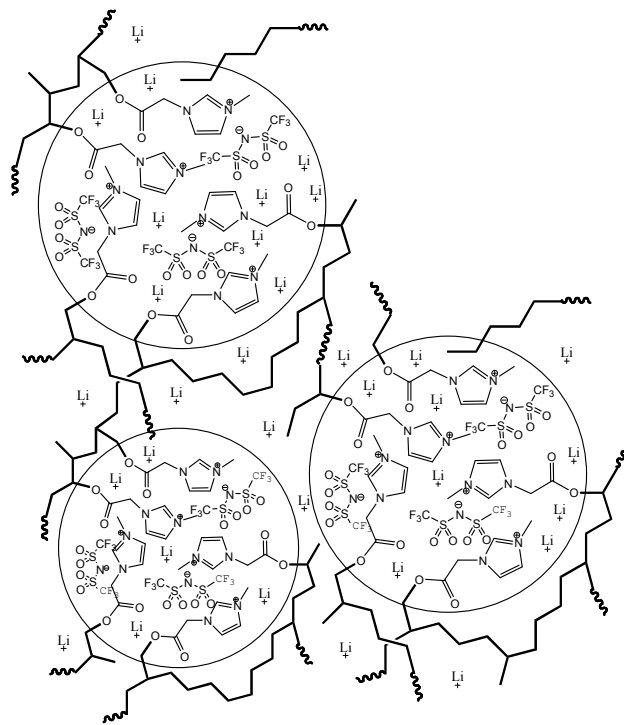
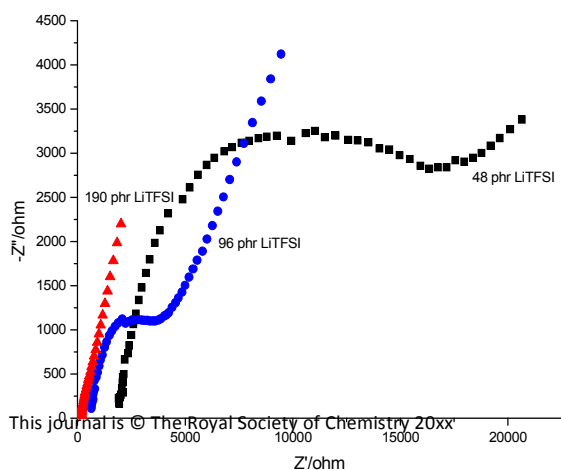
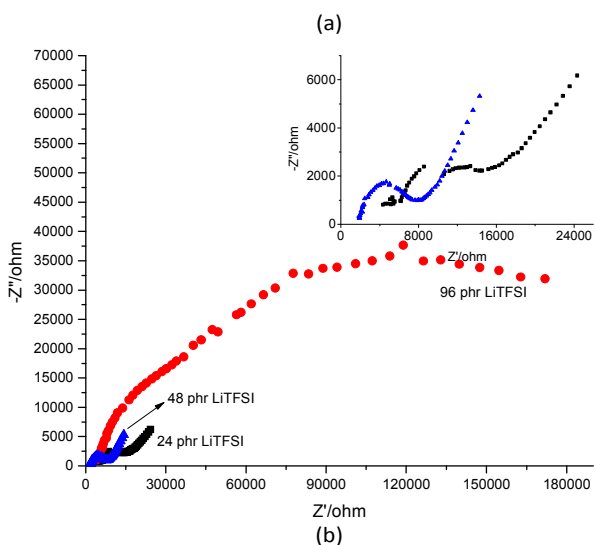
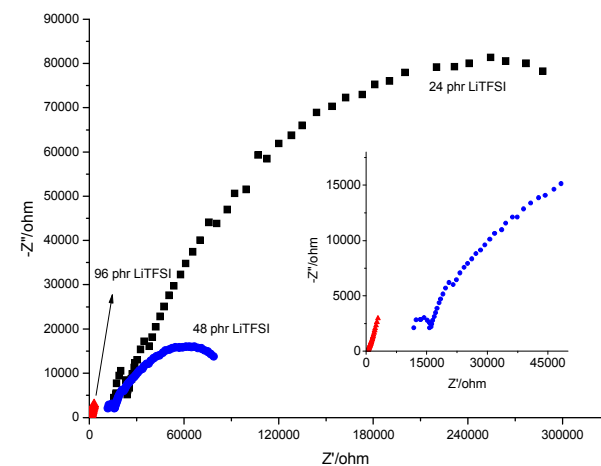
The ionic conductivity of polymer electrolyte depends on the actual concentration of the conducting species and their mobility. The intercept on the real axis of complex impedance plot of polymer electrolyte film gives the bulk resistance.³⁷ Figure 10(b) shows the complex impedance plot of ENR 50/ $[(\text{HOOC})\text{C}_1\text{C}_1\text{Im}][\text{NTf}_2]$ /LiTFSI solid electrolyte composites with 140 phr $[(\text{HOOC})\text{C}_1\text{C}_1\text{Im}][\text{NTf}_2]$ at room temperature. It consists of a high frequency semicircle and a low frequency spike. The semicircle corresponds to bulk resistance while the spike corresponds to interfacial impedance of the solid electrolyte composites. The semicircle can be represented by a parallel combination of a capacitor, which is due to the immobile polymer chain and a resistor which is due to the mobile ions inside the polymer matrix.³⁸ While some impedance spectrum of samples' semicircle is significantly broadened and the electrode spike at the low frequency end is distinctly non-vertical indicating roughness of the electrode/electrolyte interface.³⁹

The ionic conductivity of ENR 50/ $[(\text{HOOC})\text{C}_1\text{C}_1\text{Im}][\text{NTf}_2]$ /LiTFSI electrolyte composites are listed in Table 4. As shown in Table 7, the ionic conductivity depends on the concentration of $[(\text{HOOC})\text{C}_1\text{C}_1\text{Im}][\text{NTf}_2]$ and LiTFSI, and the highest conductivity ($3.01 \text{ E-}04 \text{ S cm}^{-1}$) was obtained for the sample with 190 phr LiTFSI and 280 phr $[(\text{HOOC})\text{C}_1\text{C}_1\text{Im}][\text{NTf}_2]$. Such as the samples 4, 7 and 9, the ionic conductivity of the sample containing $[(\text{HOOC})\text{C}_1\text{C}_1\text{Im}][\text{NTf}_2]$ increased 2~3 orders of magnitude when compared to the samples without $[(\text{HOOC})\text{C}_1\text{C}_1\text{Im}][\text{NTf}_2]$. As mentioned above, the ILs without chemical reactivity are used as plasticizers of solid polymer electrolyte (SPE) or gel polymer electrolytes (GPE) to improve the dispersion of LiTFSI in polymer matrix and decreasing the viscosity of polymer electrolyte composites, and then increase in ionic mobility which consequence led to increase in conductivity.^{40,41}

Nevertheless, $[(\text{HOOC})\text{C}_1\text{C}_1\text{Im}][\text{NTf}_2]$ with chemical reactivity is not only a plasticizer but also playing a vital role as a

Table 6. Mechanical properties of samples with various $[(\text{HOOC})\text{C}_1\text{C}_1\text{Im}][\text{NTf}_2]$ content

$[(\text{HOOC})\text{C}_1\text{C}_1\text{Im}][\text{NTf}_2]$ (phr)	Tensile strength (MPa)	Elongation at break (%)
35	3.44	851
70	2.16	1190
140	1.30	1057
DCP	1.61	724



(c)

Figure 10. A.C. impedance spectrum of ENR 50/ $[(\text{HOOC})\text{C}_1\text{C}_1\text{Im}][\text{NTf}_2]$ /LiTFSI solid electrolyte composites with (a) 70 phr, (b) 140 phr, (c) 280 phr $[(\text{HOOC})\text{C}_1\text{C}_1\text{Im}][\text{NTf}_2]$ at room temperature

Scheme 3. The probable mechanism of Li^+ conduction

crosslinking agent in the ENR 50/ $[(\text{HOOC})\text{C}_1\text{C}_1\text{Im}][\text{NTf}_2]$ /LiTFSI electrolyte composites, and it will be led to forming the ionic

clusters as shown in Scheme 2 in the electrolyte composites. The ionic clusters will promote the LiTFSI dissociation, and provide effective paths for migration of the lithium ions (Li^+). The probable mechanism of ionic conduction of the ENR 50/[(HOOC) $\text{C}_1\text{C}_1\text{Im}$][NTf₂]/LiTFSI electrolyte composites is drawn in Scheme 3 and the Li^+ maybe could be moved between ionic clusters under the influence of the thermodynamic movement of ENR 50-[(HOOC) $\text{C}_1\text{C}_1\text{Im}$][NTf₂] graft polymer chains.

ENR 50-[(HOOC) $\text{C}_1\text{C}_1\text{Im}$][NTf₂] hybrid material were prepared by grafting reaction of ENR 50 with [(HOOC) $\text{C}_1\text{C}_1\text{Im}$][NTf₂]. The grafting reaction and cross-linked structure of the hybrid material were investigated using the ATR-FTIR, DSC and Equilibrium swelling method. The results indicated that the carboxyl group of [(HOOC) $\text{C}_1\text{C}_1\text{Im}$][NTf₂] can react with the epoxy group of ENR 50 and generated ENR 50-[(HOOC) $\text{C}_1\text{C}_1\text{Im}$][NTf₂] graft polymer at the condition of 40 °C for 24 h. Furthermore, the grafting polymer formed ionic

4. Conclusions

Table 7. The Ionic conductivity of ENR 50/[(HOOC) $\text{C}_1\text{C}_1\text{Im}$][NTf₂]/LiTFSI solid electrolyte composites

No.	ENR 50 (phr)	[(HOOC) $\text{C}_1\text{C}_1\text{Im}$][NTf ₂] (phr)	LiTFSI (phr)	σ (S cm ⁻¹)
1	100	0	48	7.60E-08
2	100	70	24	1.66E-06
3	100	70	48	1.64E-06
4	100	70	96	1.06E-06
5	100	140	24	3.61E-06
6	100	140	48	3.95E-06
7	100	140	96	3.53E-06
8	100	280	48	1.23E-05
9	100	280	96	1.31E-05
10	100	280	190	3.01E-04

clusters and led to ionic crosslinking, which leading to a large increase of T_g and mechanical properties. From the kinetic analysis, The apparent activation energy (E) and Arrhenius frequency factor (A) obtained by the multiple-heating-rate models showed dependence on the [(HOOC) $\text{C}_1\text{C}_1\text{Im}$][NTf₂] content and the heating rate. However, with increasing [(HOOC) $\text{C}_1\text{C}_1\text{Im}$][NTf₂] content, the side group in grafted ENR 50 increase and the chains regularity are reduced, thereby the ionic crosslinking will be inhibited. In addition, ENR 50/[(HOOC) $\text{C}_1\text{C}_1\text{Im}$][NTf₂]/LiTFSI electrolyte composites were prepared through introducing LiTFSI into the ENR 50/[(HOOC) $\text{C}_1\text{C}_1\text{Im}$][NTf₂] hybrid system and the ionic conductivity of the electrolyte composites were studied. The results showed that the electrolyte composites have high ionic conductivity and reached a maximum ionic conductivity of 3.01 E-04 S cm⁻¹ (23 °C).

Acknowledgements

The authors would like to extend their sincere appreciation to the National Nature Science Foundation of China (Grant No.: 51373095).

Notes and references

- Glasse, M. D., Idris, R., Latham, R. J., Linford, R. G., & Schlindwein, W. S., *Solid State Ionics*, 2002, 147(3): 289-294.
- Shin J H, Henderson W A, Passerini S., *Electrochemistry Communications*, 2003, 5(12): 1016-1020.

- Yun-Sheng Ye, John Rick, Bing-Joe Hwang, *J Mater Chem A*, 2013, 1(8): 2719-2743.
- Welton T., *Chem. Rev.*, 1999, 99(8): 2071-2084.
- Jain, N., Kumar, A., Chauhan, S., & Chauhan, S. M. S., *Tetrahedron*, 2005, 61(5): 1015-1060.
- Fei, Z., Geldbach, T. J., Zhao, D., & Dyson, P. J., *Chemistry-A European Journal*, 2006, 12(8): 2122-2130.
- Shin J H, Henderson W A, Passerini S., *Journal of the Electrochemical Society*, 2005, 152(5): A978-A983.
- Appetecchi, G. B., Kim, G. T., Montanino, M., Carewska, M., Marcilla, R., Mecerreyes, D., & De Meazza, I., *Journal of Power Sources*, 2010, 195(11): 3668-3675.
- Goujon, L. J., Khaldi, A., Maziz, A., Plesse, C., Nguyen, G. T., Aubert, P. H., Vidal, F., Chevrot, C., Teyssié, D., *Macromolecules*, 2011, 44(24): 9683-9691.
- Zhang, Q., Li, M., Ren, W., & Zhang, Y., *Journal of Macromolecular Science, Part B*, 2012, 51(6): 1041-1048.
- Li, M., Ren, W., Zhang, Y., & Zhang, Y., *Journal of Applied Polymer Science*, 2012, 126(1): 273-279.
- Chen, J. S., Ober, C. K., Poliks, M. D., Zhang, Y., Wiesner, U., & Cohen, C., *Polymer*, 2004, 45(6): 1939-1950.
- J. Brandrup, E.H. Immerjat (Eds.), *Wiley*, New York, 1989, p. 1175 (Section VII).
- Mertzel E, Koenig J L., *Springer Berlin Heidelberg*, 1986: 73-112.
- Noor, S. A. M., Ahmad, A., Talib, I. A., & Rahman, M. Y. A., *Ionics*, 2010, 16(2): 161-170.
- Dorbritz S, Ruth W, Kragl U., *Adv. Synth. Catal.*, 2005, 347(9): 1273-1279.
- Feng, Q., Wang, H., Zhang, S., & Wang, J., *Colloids and Surfaces A: Physicochemical and Engineering Aspects*, 2010, 367(1): 7-11.
- Sato K., *Rubber chemistry and technology*, 1983, 56(5): 942-958.

- 19 Holiday L., London: Applied Science Publisher, 1975, Cha 3
- 20 Eisenberg A, Hird B, Moore R B., *Macromolecules*, 1990,23 (18): 4098-4107
- 21 Khokhlov A R, Dormidontova E E. *Physics-Usppekhi*, 1997, 40(2): 109-124.
- 22 Gan S N, Burfield D R. Dsc studies of the reaction between epoxidized natural rubber and benzoic acid [J]. *Polymer*, 1989, 30(10): 1903-1908.
- 23 Lu M C, Hong J L. Cure kinetics and gravimetric analysis of a flexible aromatic dicyanate, cyanated phenylene sebacate oligomer [J]. *Polymer*, 1994, 35(13): 2822-2827.
- 24 Ozawa T. Kinetics of non-isothermal crystallization [J]. *Polymer*, 1971, 12(3): 150-158.
- 25 Flynn J H, Wall L A. A quick, direct method for the determination of activation energy from thermogravimetric data [J]. *Journal of Polymer Science Part B: Polymer Letters*, 1966, 4(5): 323-328.
- 26 Kissinger H E. Reaction kinetics in differential thermal analysis [J]. *Analytical chemistry*, 1957, 29(11): 1702-1706.
- 27 Montserrat S, Málek J. A kinetic analysis of the curing reaction of an epoxy resin[J]. *Thermochimica acta*, 1993, 228: 47-60.
- 28 Crane, L. W. *J Polym Sci Polym Lett Ed* 1973, 11, 533.
- 29 Teo J K H, Teo K C, Pan B, et al. Epoxy/polyhedral oligomeric silsesquioxane (POSS) hybrid networks cured with an anhydride: Cure kinetics and thermal properties [J]. *Polymer*, 2007, 48(19): 5671-5680.
- 30 Xu W, Bao S, Shen S, et al. Differential scanning calorimetric study on the curing behavior of epoxy resin/diethylenetriamine/organic montmorillonite nanocomposite [J]. *Journal of Polymer Science Part B: Polymer Physics*, 2003, 41(4): 378-386.
- 31 Omidian H, Hasherni S A, Askari F, et al. Swelling and crosslink density measurements for hydrogels [J]. *Iranian J. of Polymer Science and Technology Vol*, 1994, 3(2).
- 32 El-Sabbagh S H, Yehia A A. Detection of crosslink density by different methods for natural rubber blended with SBR and NBR [J]. *Egyptian Journal of Solids*, 2007, 30(2): 157-173.
- 33 Scott R A, Peppas N A. Compositional effects on network structure of highly cross-linked copolymers of PEG-containing multiacrylates with acrylic acid [J]. *Macromolecules*, 1999, 32(19): 6139-6148.
- 34 De Yao K, Liu J, Cheng G X, et al. Swelling behavior of pectin/chitosan complex films [J]. *Journal of applied polymer science*, 1996, 60(2): 279-283.
- 35 Sae-oui P, Sirisinha C, Thepsuwan U, et al. Dependence of mechanical and aging properties of chloroprene rubber on silica and ethylene thiourea loadings[J]. *European Polymer Journal*, 2007, 43(1): 185-193.
- 36 Marzec A, Laskowska A, Boiteux G, et al. The impact of imidazolium ionic liquids on the properties of nitrile rubber composites [J]. *European Polymer Journal*, 2014, 53: 139-146.
- 37 Rajendran S, Sivakumar M, Subadevi R. Li-ion conduction of plasticized PVA solid polymer electrolytes complexed with various lithium salts [J]. *Solid State Ionics*, 2004, 167(3): 335-339.
- 38 Ramesh S, Arof A K. Ionic conductivity studies of plasticized poly (vinyl chloride) polymer electrolytes [J]. *Materials Science and Engineering: B*, 2001, 85(1): 11-15.
- 39 Venkateswarlu M, Reddy K N, Rambabu B, et al. Ac conductivity and dielectric studies of silver-based fast ion conducting glass system [J]. *Solid State Ionics*, 2000, 127(1): 177-184.
- 40 Baskaran R, Selvasekarapandian S, Kuwata N, et al. Conductivity and thermal studies of blend polymer electrolytes based on PVAc-PMMA [J]. *Solid State Ionics*, 2006, 177(26): 2679-2682.
- 41 Lu G, Li Z F, Li S D, et al. Blends of natural rubber latex and methyl methacrylate-grafted rubber latex [J]. *Journal of applied polymer science*, 2002, 85(8): 1736-1741.